Songklanakarin J. Sci. Technol.
34 (6), 629-636, Nov. - Dec. 2012

SJST SONGKLANAKARIN JOURNAL OF SCIENCE AND TECHNOLOGY
http://www.sjst.psu.ac.th

Original Article

Performance analysis of linear bandpass filter and pulse inversion in separating subharmonic frequency of signals from ultrasound contrast agent

Chinda Samakee* and Pornchai Phukpattaranont

Department of Electrical Engineering, Faculty of Engineering
Prince of Songkla University, Hat Yai, Songkhla, 90112 Thailand.

Received 19 October 2011; Accepted 10 October 2012

Abstract

Recently, many publications reported the generation of subharmonic frequency ($f_0/2$) and its potential use in imaging from ultrasound contrast agent (UCA). Subharmonic imaging (SHI) has provided better contrast resolution over the second harmonic signals due to the lack of subharmonic generation in the tissue region. However, subharmonic separation in SHI utilizes linear bandpass filtering only. In this paper, we compare the subharmonic separation capability of linear band filter (LBF), pulse inversion (PI), and their combination (PILBF) based on contrast-to-tissue ratio (CTR). Results show that the CTR values from the LBF, the PI, and the PILBF are 20.30, 40.30, and 52.74 dB, respectively. The optimal stopband attenuation and fractional bandwidth for the PILBF method are 50 dB and 10%, respectively. This high CTR value indicates the feasibility of the PILBF method in creating high quality ultrasound image from subharmonic frequency.

Keywords: subharmonic, linear bandpass filter, pulse inversion, ultrasound contrast agent

1. Introduction

Nowadays, ultrasound contrast agent (UCA) is widely used for the improving diagnostic capabilities of medical ultrasound in clinical applications (Calliada *et al*., 1998; Cosgrove, 2006). Various applications of UCA include perfusion estimation and blood vessel detection. Moreover, UCA is not only useful for ultrasound imaging, but also is an important tool for drug delivery (Harvey *et al*., 2002; Jiang *et al*., 2009). UCA is an external substance containing free gas or encapsulated microbubble with size diameter between 1 and 10 μm to allow passage of the lung capillaries. They oscillate under insonation, thus enhancing backscatter signals from blood and improving the visualization of blood from the surrounding medium (De Jong *et al*., 2002a, De Jong *et al*., 2009). In addition, the nonlinear interaction between UCA and ultrasound wave can generate fundamental (f_0) and higher multiple frequencies ($2f_0$, $3f_0$, $4f_0$, ...) (De Jong *et al*., 1994a,b; Hann *et al*., 1999; Jang *et al*., 2000; Averkiou, 2000). The contrast-to-tissue ratio (CTR) can be further improved by separating the second harmonic frequency ($2f_0$) from the fundamental frequency (f_0) signals e.g. in harmonic imaging (HI) (De Jong *et al*., 2000; De Jong *et al*., 2002b; Kollmann, 2007; Nimanee *et al*., 2007) and pulse inversion (Simpson *et al*., 1999). However, HI suffers from reduced CTR due to second harmonic generation and accumulation within the tissue region, especially the excitation at high mechanical index (MIs) (Forsberg *et al*., 2000).

Recent research has reported the generation of subharmonic frequency ($f_0/2$) and a view towards potential use in subharmonic imaging (SHI) of signals from UCA (Forsberg, *et al*., 2000; Forsberg *et al*., 2007; Eisenbrey *et al*., 2011). Shankar *et al*. (1998) reported significant amounts of subharmonic signals from UCA that provided better CTR over the second harmonic signals due to the lack of subharmonic signals generated by the surrounding tissues. Ongoing research in this area can be categorized into two directions: the optimization for subharmonic generation and the optimi-

* Corresponding author.
Email address: chindasamakee@hotmail.com

zation for subharmonic separation. The publications on subharmonic generation include Krishna *et al.* (1999); Shanker *et al.* (1999); Yanjun *et al.* (2005); YanJun *et al.* (2006); Zhang *et al.* (2007); and Zhang *et al.* (2009). On the other hand, in order to improve CTR values, digital signal processing applications such as filtering in SHI are used for separating subharmonic components. However, the application of pulse inversion (PI), which is well known for second harmonic separation, has not been studied for subharmonic separation. Therefore, we propose to study and compare the performance of subharmonic separation capability of linear band filter (LBF), pulse inversion (PI), and their combination, pulse inversion linear band filter (PILBF), in this paper.

The paper is organized as follows. The theory of subharmonic simulation and the principles of LBF, PI and PILBF for subharmonic separation are presented in Section 2. Section 3 gives a description of the simulation methods for subharmonic generation, subharmonic separation, and the measurement of capability in separating subharmonic components. Results and discussion are provided in Section 4. Finally, conclusions are drawn in Section 5.

2. Theory

In this section, the theory and principles of subharmonic simulation based on the Church's model are described. Then, the theories and principles of three subharmonic separation techniques used in this paper are provided. Details are as follows.

2.1 Subharmonic simulation

The subharmonic simulation from the oscillation behavior of encapsulated microbubble is described by Church's model. The validity of the model is verified with the agreement between the experimental measurement and theoretical predictions (YanJun *et al.*, 2006). The Church equation for encapsulated microbubble can be expressed as (YanJun *et al.*, 2005; Zhang *et al.*, 2007; Zhang *et al.*, 2009)

$$\rho_L\left(R''R+\frac{3}{2}(R')^2\right)=p_0\left(\left(\frac{R_0}{R}\right)^{3\kappa}-1\right)-p_i(t)-4\mu_L\frac{R'}{R}-12\mu_s\frac{d_sR_0^2}{R^3}\frac{R'}{R}-12G_s\frac{d_sR_0^2}{R}\left(1-\frac{R_0}{R}\right), \tag{1}$$

where R is the instantaneous radius of the bubble, R', R'' are the first and second time derivatives of instantaneous radius, respectively; R_0 is the equilibrium radius. For the surrounding liquid, ρ_L and μ_L are the density and shear viscosity, respectively. For the bubble shell, d_s is the shell thickness at rest; μ_s is the shear viscosity of the surface and G_s is the shear modulus. κ is the polytropic exponent. p_0 is the hydrostatic pressure. $p_i(t)=p_A cos(\omega t)$ is the time-varying excitation acoustic pressure; p_A is amplitude pressure; ω is the angular frequency. The level of subharmonic generation is dependent on the resonance frequency (f_r) of the encapsulated bubble, which is given by

$$f_r=\frac{\omega}{2\pi}=\frac{1}{2\pi R_0}\sqrt{\frac{1}{\rho_L}\left(3\kappa p_0+12G_s\frac{d_s}{R_0}\right)}, \tag{2}$$

When the radius of oscillation behavior is calculated and known, the sound pressure ($P_C(t)$) can be expressed as (Morgan, *et al.*, 2000)

$$P_C(t)=\rho_L r^{-1}\left(R^2R''+2R(R')^2\right). \tag{3}$$

where r is the distance between a sensor and a target. In addition, an additive Gaussian white noise is added to all acoustic pressure signals $p_i(t)$ to achieve a signal-to-noise ratio of 50 dB.

2.2 Subharmonic separation

The techniques used for separating subharmonic frequency are linear bandpass filter (LBF) method, pulse inversion (PI) method, and combination of the PI and the LBF (PILBF). Details of each method are described below.

2.2.1 The LBF method

A finite-impulse response (FIR) linear bandpass filter is used in separating subhamonic frequency because the FIR filter is exactly linear phase and inherently stable (Mitra, 2006). We design the LBF based on the Parks-McClellan algorithm, which affords the best control over band limits and high stopband attenuations. The LBF parameters to be optimized are fraction bandwidth (*FB*) and stopband attenuation (*SA*). The optimal LBF should enhance subharmonic component of echoes from UCA and separate UCA signals from tissue signals. Two parameters of the LBF are varied in the design to achieve the best filter for improving subharmonic separation in terms of CTR. The *FB* of the LBF can be obtained by (Nimanee *et al.*, 2007)

$$FB=\frac{2f_B}{f_C}\times 100\%, \tag{4}$$

where *FB* is a fraction bandwidth, f_B is an one-half of passband duration defined in the filter specification and f_C is a center frequency. Moreover, *SA* is defined in terms of dB below the passband of the filter.

2.2.2 The PI method

In the PI method, two ultrasound waves are sent into the medium region. The second wave is inverted (i.e. 180 degree phase shifted and sent after a suitable delay) with respect to the first wave. Afterwards, the two echo sequences from UCA region are summed, which are not totally cancelled to be zero for nonlinear echoes. However, for linear echoes from tissue region, the sum of two inverted signals is zero (Simpson *et al.*, 1999).

2.2.3 The PILBF Method

The PILBF method combines between the PI and the LBF due to the advantage of PI method that can remove the fundamental frequency better than the LBF method. We designed the LBF from yielded output signals of the PI. For more details of the design can be seen in Samakee and Phukpattaranont (2011b).

3. Materials and Methods

3.1 Subharmonic simulation

The simulation of subharmonic generation was implemented by numerical solution of the Church equation. The parameters are as follows: $R_0 = 1.5\times10^{-6}$, $d_s = 0.1\%\times R_0$ μm, $G_s = 10$ MPa, $\rho_L = 1000$ kg·m^{-3}, $r_0 = 1.01\times10^5$ Pa, $\mu_L = 0.001$ Pa·s, $\mu_S = 1.49$ Pa·s and $\kappa = 1.09$. The radius is obtained from the numerical solution of equation (1) using an explicit fourth-order Rung-Kutta algorithm at a sampling frequency 60 MHz. The initial values are $R = R_0$ and $R' = 0$ at $t = 0$. For the bubble with a radius of 1.5 μm, the resonance frequency calculated by equation (2) is about 2.25 MHz. The excitation amplitude pressure is 0.6 MPa. The transmit frequency is about $f = 2f_r$ (4.5 MHz) with time duration of 40 μs, which is optimal for subharmonic generation (Samakee and Phukpattaranont, 2011c). After the oscillation is calculated, the sound pressure is computed with the distance $r = 6$ cm. In addition, the tissue echo ($P_T(t)$), which is used as a reference, is given by

$$P_T(t) = \frac{P_{C(\max)}}{p_{i(\max)}} \times p_i(t), \tag{5}$$

where $P_{C(max)}$ and $p_{i(max)}$ are the peak amplitude value of an UCA echo and the acoustic input pressure, respectively.

3.2 Subharmonic separation

3.2.1 The LBF method

Figure 1 shows the block diagram of subharmonic separation using the LBF method. The input wave $p_i(t)$ is sent into the Church's model. Then, the instantaneous radius $R(t)$ of bubble and predicted echo $P_C(t)$ is produced. In filtering process, the $P_C(t)$ signal is filtered by the LBF for separating subharmonic component from UCA echoes. P_F is the output signal after filtering with the LBF. To investigate the optimal *SA*, the *FB* is fixed at 12.5% and the *SA* is varied between 30 and 50 dB. Subsequently, the *SA* is fixed at 50 dB and the *FB* is varied between 10 and 50% to investigate the optimal *FB*. In Samakee and Phukpattaranont (2011a) we have reported more details of this LBF design.

3.2.2 The PI method

Figure 2 shows the block diagram of subharmonic separation using the PI method. The first wave $p_1(t)$ is sent into the Church's model. Then, the instantaneous radius $R_1(t)$ of bubble and predicted echo $P_{C1}(t)$ is produced. Afterwards, the second wave $p_2(t)$ is sent with inverted phase of the first wave. The instantaneous radius $R_2(t)$ and predicted echo $P_{C2}(t)$ is produced. The output signal P_{sum} of the PI method can be obtained from the sum of $P_{C1}(t)$ and $P_{C2}(t)$.

3.2.3 The PILBF method

To compare performance of the PILBF with the LBF, the *SA* and the *FB* are varied in a similar way as described in Section 3.2.1. In other words, the *FB* is fixed at 12.5% and the *SA* is varied between 20 and 50 dB. Subsequently, the *SA* is fixed at 50 dB and the *FB* is varied between 10 and 50%.

3.3 Performance measurement

The measurement of capability in separating subharmonic component from tissue echo using a contrast-to-tissue ratio (CTR) is given by Phukpattaranont and Ebbini (2003)

$$CTR = 10\log\frac{\overline{P}_C}{\overline{P}_T}, \tag{6}$$

where $\overline{P}_C$ and $\overline{P}_T$ are the average power of signals in UCA and tissue regions, respectively. The higher CTR value confirms the better capability in separating subharmonic component.

4. Results and Discussion

4.1 Subharmonic simulation

Figure 3 shows spectra of signals from UCA and tissue regions. The analysis of power spectrum is from the use of fast Fourier transform (FFT) with a Hamming window. We used 600 points of data with zero padding to 2400 points. On the one hand, the power spectrum of UCA signal (thick

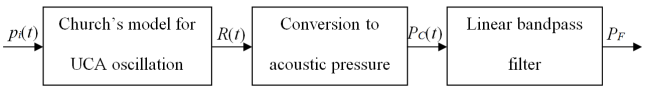

Figure 1. The block diagram of subharmonic separation using the LBF method.

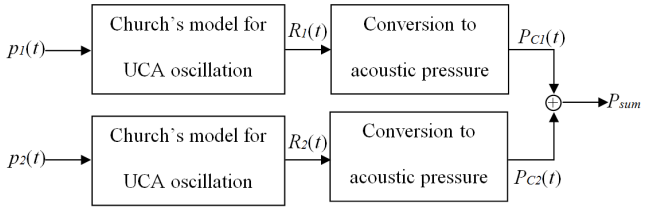

Figure 2. The block diagram of subharmonic separation using the PI method.

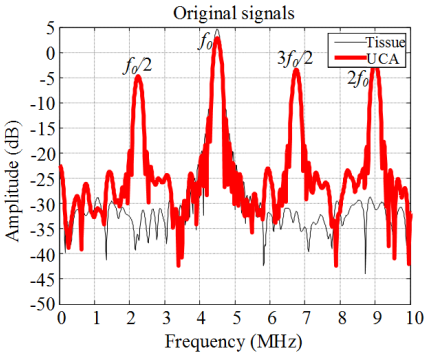

Figure 3. Power spectra of signals from UCA (thick line) and tissue (thin line) regions before processing. The CTR value is -2.59 dB.

line) indicates the various nonlinear components, i.e. subharmonic ($f_0/2$), fundamental (f_0), ultraharmonic ($3f_0/2$) and higher multiple ($2f_0$) frequencies. On the other hand, the power spectrum of the tissue signal (thin line) shows a fundamental (f_0) frequency only. In addition, the CTR value is -2.59 dB.

4.2 The LBF method

4.2.1 *SA* variation

We designed the LBF with a fixed *FB* of 12.5% in order to investigate the appropriate *SA*. Power spectra of signals after filtering produced from the *SA* of 30, 40, 50 and 60 dB are shown in Figure 4(a), (b), (c), and (d), respectively. In addition, the calculations of CTR values of signals in Figure 4(a)-(d) are 9.80, 17.44, 19.43 and 18.99 dB, respectively. The LBFs with the *SA* from 40 to 60 dB give high CTR values, which are appropriate to be used in separating the subharmonic component.

4.2.2 *FB* variation

We designed the LBF with a fixed *SA* of 50 dB in order to investigate the appropriate *FB*. Power spectra of signals after filtering with the LBF produced from the *FB* of 10%, 15%, 25%, and 50% are shown in Figure 5(a), (b), (c) and (d), respectively. The CTR values of signals in Figure 5(a)-(d) are 20.30, 17.95, 17.03 and 13.32 dB, respectively. The appropriate *FB* for subharmonic separation is between 10% and 25%.

4.3 The PI method

Figure 6 shows the power spectra of signals from UCA and tissue using the PI method. We can see the good suppression of fundamental frequency in signals from both regions. However, the PI cannot remove ultraharmonic and second harmonic components. In addition, the CTR value of signal in Figure 6 is 40.30 dB.

4.4 The PILBF method

4.4.1 *SA* variation

We have output signals from the PI method, which is introduced into the LBF for separating subharmonic compo-

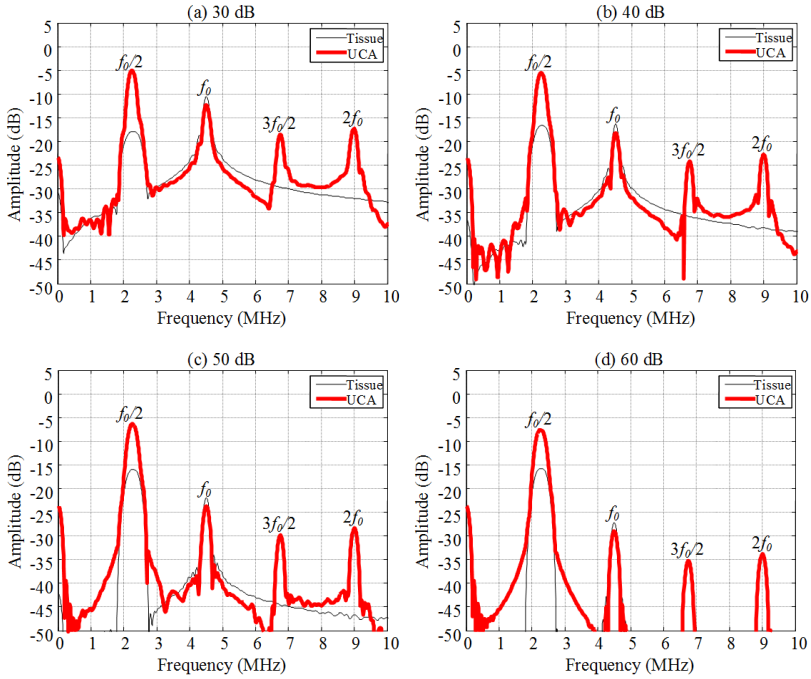

Figure 4. Power spectra of signals after filtering with the LBF by varying *SA* to be 30, 40, 50, and 60 dB. *FB* is fixed at 12.5%. The CTR values of signals in Figure 4(a), (b), (c), and (d) are 9.80, 17.44, 19.43, and 18.99 dB, respectively.

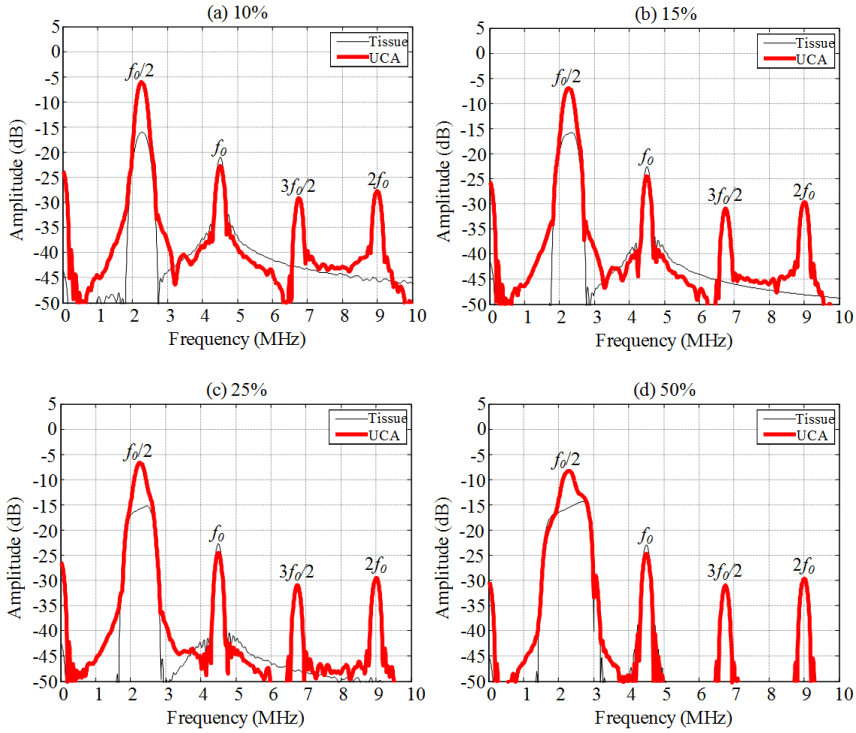

Figure 5. Power spectra of signals after filtering with the LBF by varying *FB* to be 10%, 15%, 25%, and 50%. *SA* is fixed at 50 dB. The CTR values of signals in Figure 5(a), (b), (c), and (d) are 20.3, 17.95, 17.03, and 13.32 dB, respectively.

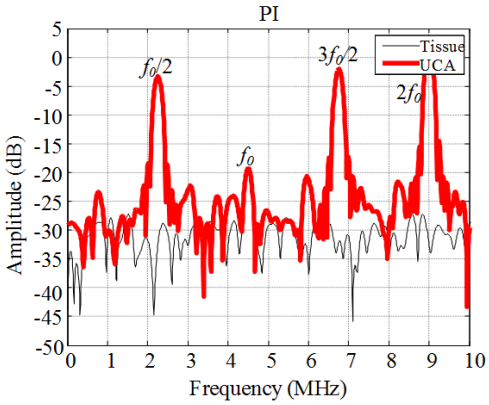

Figure 6. Power spectra of signals after processing with the PI method. The CTR value is 40.30 dB.

nent. We used the center frequency at 2.25 MHz for designing the LBF on PI data by varying the *SA* and *FB*. We begin varying the *SA* of 20 dB with the *FB* fixed at 12.5%. Power spectrum of output signal after filtering is shown in Figure 7(a). The calculation of CTR value for signals in Figure 7(a) is 47.71 dB. At the *SA* 30 dB, the CTR value increases to 50.73 dB as shown in Figure 7(b). Result of the *SA* at 40 dB is shown in Figure 7(c). The CTR value of signals in Figure 7(c) is 51.27 dB. When the *SA* increases to 50 dB as shown in Figure 7(d), the CTR value of signals in Figure 7(d) is 51.09 dB. The results of PILBFs with the *SA* between 30 dB and 50 dB give high CTR values and are appropriate to be used in separating the subharmonic component.

4.4.2 *FB* variation

We select a fixed *SA* value at 50 dB and vary the *FB* to 10%, 15%, 25% and 50%. Power spectra of signals after filtering with the PILBFs are shown in Figure 8(a), (b), (c) and (d), respectively. In addition, the CTR values of signals in Figure 8(a)-(d) are 52.74, 49.11, 48.51, and 46.10 dB, respectively. The results of PILBFs with the *FB* between 10% and 25% provide the high CTR values, which are appropriate for separating the subharmonic component.

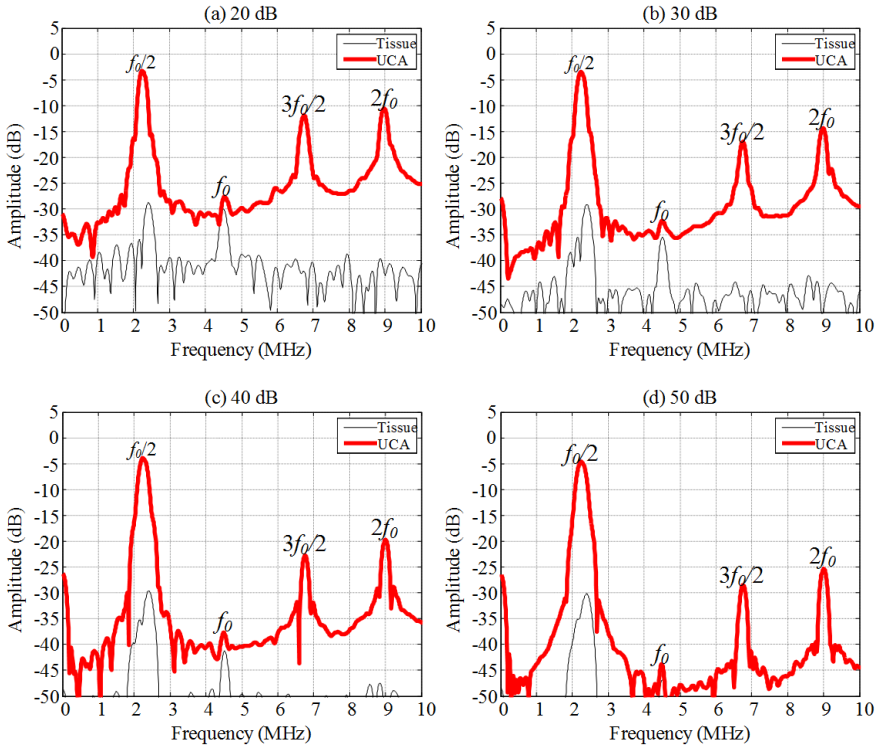

Figure 7. Power spectra of signals after processing with the PILBF by varying *SA* to be 20, 30, 40, and 50 dB. *FB* is fixed at 12.5%. The CTR values of signals in Figure 7(a), (b), (c), and (d) are 47.71, 50.73, 51.27, and 51.09 dB, respectively.

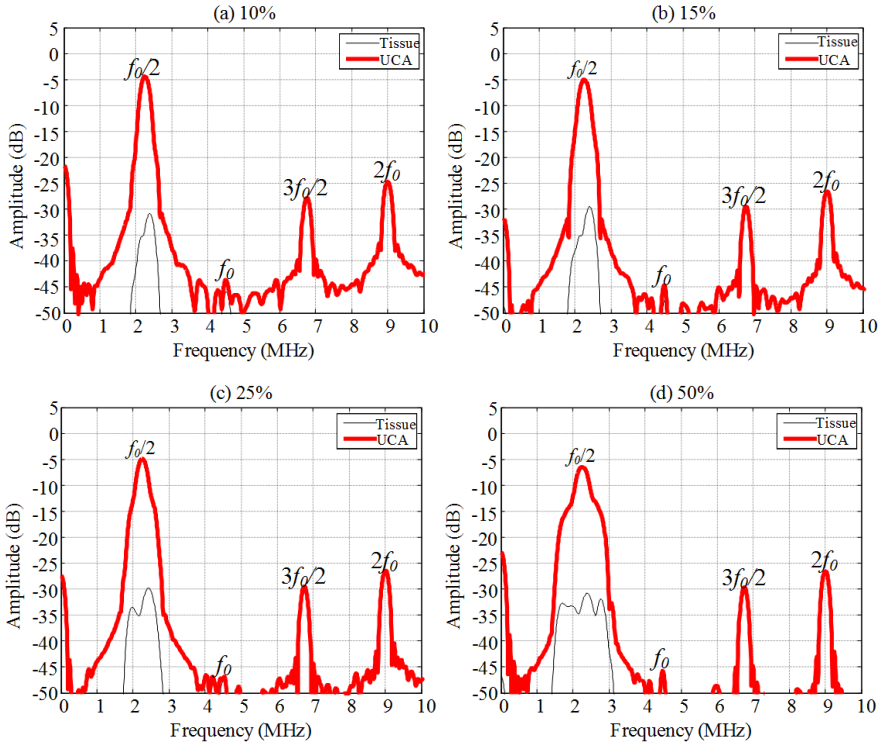

Figure 8. Power spectra of signals after processing with the PILBF by varying *FB* to be 10%, 15%, 25%, and 50%. *SA* is fixed at 50 dB. The CTR values of signals in Figure 8(a), (b), (c), and (d) are 52.74, 49.11, 48.51, and 46.10 dB.

4.5 Comparison of performance measurement

The capability of separating subharmonic component obtained from the LBF, the PI and the PILBF give different CTR values. The CTR value of the original signals without processing is -2.59 dB. The LBF produced by filtering the simulation data provides the highest CTR value of 20.30 dB with *SA* 50 dB and *FB* 10%. The PI method can improve the CTR value up to 40.30 dB. For the PILBF method, the highest CTR value is 52.74 dB obtained with the appropriate *SA* and *FB* values of 50 dB and 10%, respectively. The maximum CTR value from the PILBF method is 52.74 dB, which is better than the original signal, the LBF and the PI method.

5. Conclusions

We demonstrated the techniques' capability in separating subharmonic component from UCA nonlinear signals using LBF, PI and PILBF in terms of CTR values. The results indicated that the CTR value from the PILBF (52.74 dB) is the highest compared to the PI (40.30 dB), the LBF (20.30 dB) and the conventional (-2.59 dB) techniques. The capability of the PILBF in improving the CTR values guarantees the creation of high quality subharmonic imaging in diagnostic ultrasound.

Acknowledgement

This research project was financially supported by the Faculty of Engineering, Prince of Songkla University, Thailand.

References

Averkiou, M.A. 2000. Tissue harmonic imaging. Proceedings of the Institute of Electrical and Electronics Engineers International Ultrasonics Symposium. p.1563-1572.

Calliada, F., Campani, R., Bottinelli, O., Bozzini, A., and Sommaruga, M.G. 1998. Ultrasound contrast agents basic principles. European Journal of Radiology. 27, S157-S160.

Cosgrove, D. 2006. Ultrasound contrast agents: An overview. European Journal of Radiology. 60, 324-330.

De Jong, N., Frinking, P. J.A., Bouakaz A., and Ten Cate F. J. 2000. Detection procedures of ultrasound contrast agents. Ultrasonics. 38, 87-92.

De Jong, N., Bouakaz, A., and Frinking, P. 2002a. Basic acoustic properties of microbubbles. Echocadiography. 19, 229-240.

De Jong N., Bouakaz A., and Ten Cate F. J. 2002b. Contrast harmonic imaging. Ultrasonics. 40, 567-573.

De Jong, N., Cornet, R., and Lancee, C.T. 1994a. Higher harmonics of vibrating gas filled microspheres. Part one: Simulations. Ultrasonics. 32(6), 447-453.

De Jong, N., Cornet, R., and Lancee, C.T. 1994b. Higher harmonics of vibrating gas filled microspheres. Part two: Measurements. Ultrasonics. 32(6), 455-459.

De Jong, N., Emmer M., Van Wamel A., and Versluis M. 2009. Ultrasonic characterization of ultrasound contrast agents. Medical & Biological Engineering & Computing. 47, 861-873.

Eisenbrey, J.R., Dave, J.K., Halldorsdottir, V.G., Merton, D.A., Machado, P., Liu, J.B., Miller, C., Gonzalez, J.M., Park, S., Dianis, S., Chalek, C.L., Thomenius, K.E., Brown, D.B., Navarro, V., and Forsberg F. 2011. Simultaneous grayscale and subharmonic ultrasound imaging on a modified commercial scanner. Ultrasonics. 51, 890-897.

Forsberg, F., Shi, W.T., and Goldberg, B.B. 2000. Subharmonic imaging of contrast agents. Ultrasonics. 38, 93-98.

Forsberg, F., Piccoli, C.W., Merton, D.A., Palazzo, J.J., and Hall, A.L. 2007. Breast lesions: Imaging with contrast-enhanced subharmonic US-initial experience. Radiology. 244, 718-726.

Hann, L.E., Bach, A.M., Cramer, L.D., Siegel, D., Yoo, H.H., and Garcia R. 1999. Hepatic sonography: comparison of tissue harmonic and standard sonography techniques. American Journal of Roentgenology. 173(1), 201-206.

Harvey, C.J., Pilcher, J.M., Eckersley, R.J., Blomley, M.K., and Cosgrove, D.O. 2002. Advances in ultrasound. Clinical Radiology. 57, 157-177.

Jang, H.J., Lim, H.K., Lee, W.J., Kim, S.H., Kim, K.A., and Kim, E.Y. 2000. Ultrasonographic evaluation of focal hepatic lesions: comparison of pulse inversion harmonic, tissue harmonic, and conventional imaging techniques. Journal of Ultrasound in Medicine. 19(5), 293-299.

Jiang, Y., Zhu J., Hu Y., Xing C., Li D., and Hu B. 2009. Can scavenger receptor Class B Type I loaded ultrasound contrast agent be a new method for treating atherosclerosis?. Medical Hypotheses. 73, 36-37.

Kollmann, C. 2007. New sonographic techniques for harmonic imaging-Underlying physical principles. European Journal of Radiology. 64, 164-172.

Krishna, P.D., Shankar, P.M. and Newhouse, V.L. 1999. Subharmonic generation from ultrasonic contrast agents. Physics in Medicine and Biology. 44, 681-694.

Morgan, K.E., Allen, J.S., Dayton, P.A., Chomas, J.E., Klibanov, A.L. and Ferrara, K.W. 2000. Experimental and theoretical evaluation of microbubble behavior: effect of transmitted phase and bubble size. The Institute of Electrical and Electronics Engineers Transactions on Ultrasonics, Ferroelectrics and Frequency Control. 47(6), 1494-1509.

Nilmanee, T., Thienmontri S., Jindapetch N., and Phukpattaranont, P. 2007. Second harmonic imaging from pulse-echo signals of contrast-assisted ultrasound. Suranaree Journal of Science and Technology. 14, 323-330.

Phukpattaranont, P. and Ebbini, E.S. 2003. Post-beamforming second-order Volterra filter for pulse-echo ultrasonic imaging. The Institute of Electrical and Electronics Engineers Transactions on Ultrasonics, Ferroelectrics

and Frequency Control. 50(8), 987-1001.

Mitra, S. K. 2006. Digital Signal Processing A Computer Base Approach, McGraw-Hill, Inc., New York, U.S.A., pp. 523.

Samakee, C. and Phukpattaranont, P. 2011a. Optimal linear bandpass filter for separating subharmonic components from ultrasound contrast agents. Proceeding of the 5th on PSU-UNS. International Conference on Engineering and Technology, Phuket, Thailand, May 2-3, 2011, 439-442.

Samakee, C. and Phukpattaranont, P. 2011b. Pulse inversion linear bandpass filter for detecting subharmonic from microbubbls. Proceeding of the 2011 Eighth International Joint Conference. International Conference on Computer Science and Software Engineering, Nakhon Pathom, Thailand, May 11-13, 2011, 143-148.

Samakee, C. and Phukpattaranont, P. 2011c. Simulation of subharmonic generation based on nonlinear oscillation from ultrasound contrast agents. Proceeding of 8th on Electrical Electronics, Computer, Telecommunications and Information Technology Association. International Conference on Signal Processing, Khon Kaen, Thailand, May 17-19, 2011, 1015-1018.

Shankar, P.M., Krishna, P.D., Newhouse, V.L. 1998. Advantages of subharmonic over second harmonic backscatter for contrast-to-tissue echo enhancement. Ultrasound in Medicine & Biology. 24(3), 395-399.

Shankar, P.M., Krishna, P.D. and Newhouse, V.L. 1999. Subharmonic blackscattering from ultrasound contrast agents. Journal of the Acoustical Society of America. 106(4), 2104-2110.

Simpson, D.H., Chin, C.T., and Burns, P.N. 1999. Pulse inversion Doppler: A new method for detecting nonlinear echoes from microbubble contrast agents. The Institute of Electrical and Electronics Engineers Transactions on Ultrasonics, Ferroelectrics and Frequency Control. 46(2), 372-382.

Yanjun, G., Dong, Z. and Xiufen, G. 2005. Subharmonic and ultraharmonic emissions based on the nonlinear oscillation of encapsulated microbubbles in ultrasound contrast agents. Chinese Science Bulletin. 50, 1975-1978.

Yanjun, G., Dong, Z., Xiufen, G., Kaibin, T. and Zheng, L. 2006. The viscoelasticity of lipid shell and the hysteresis of subharmonic in containing microbubbles. Chinese Physics Society. 15(7), 1526-1531.

Zhang, D., Gong, Y., Gong, X., Liu, Z., Tan, K. and Zheng, H. 2007. Enhancement of subharmonic emission from encapsulated microbubbles by using a chirp excitation technique. Physics in Medicine and Biology. 52, 5531-5544.

Zhang, D., Xi, X., Zhang, Z., Gong, X., Chen, G. and Wu, J. 2009. A dual-Frequency excitation technique for enhancing the sub-harmonic emission from encapsulated microbubbles. Physics in Medicine and Biology. 54, 4257-4272.